International Journal of Fracture Fatigue and Wear, Volume 2

Proceedings of the 3rd International Conference on
Fracture Fatigue and Wear, pp. 269-274, 2014

ON FRETTING FATIGUE BEHAVIOUR OF SINGLE BOLTED LAP JOINT

R. Hojjati-Talmei[1,2], M.A. Wahab[1] T. Yue[1] and L. D'Alvise[2]

[1]Department of Mechanical Construction and Production, Faculty of Engineering and Architecture, Ghent University, Belgium
[2] Geonx Inc., Gosselies, Belgium

Abstract: Fretting fatigue failure mechanisms occurs between connected parts which are subjected to small oscillatory relative movement and bulk fatigue loading condition at the same time. In this study, fretting fatigue behaviour of single bolted lap joint connection is investigated by means of finite element modelling approach. To this end, a 3-D finite element model was developed to characterize behaviour of single bolted joint subjected to fretting fatigue loading conditions, which consists of initial crack site estimation, stress and slip distribution at contact interface.

Keywords: DIC; fretting fatigue; SBLJ; slip amplitude

1 INTRODUCTION

Fretting fatigue failure evolution is caused by combination of several parameters, which can be related to different mechanical response of material. These parameters can be divided into two sets of primary and secondary variables, which have more and less influence on fretting fatigue total lifetime. In general, fretting fatigue failure process is divided into two main phases, namely crack initiation and crack propagation. The fraction of fretting fatigue lifetime spent in crack initiation and in crack propagation depends on many factors, e.g. contact stresses, amount of slip, frequency, environmental conditions, etc., and varies from one practical application to another. Numerical modelling techniques are proper toolkits for analyzing fretting fatigue behaviour of contact problems subjected to fretting fatigue loading condition.

The early Finite Element Analysis (FEA) study of riveted joints dates back to mid-90's reported by Hoeppner et al. [1]. When a FEA based methodology was used to determine the stress state at rivet locations, where the fretting fatigue crack initiates. They used the FEA results as a valid baseline condition to apply the method for prediction of Coefficient of Friction (COF) during fretting process to a riveted joint. Szolwinski et al. [2] targeted at characterizing the conditions at/around the rivet/hole interface by means of FEA approach. They modelled both mechanics of load transfer in riveted joints and the residual stress field. A 3-D FEA of riveted joint was modelled by Guo et al. [3]. They have tried to study the mechanism of fretting fatigue crack formation in aluminium alloys, and the determination of the characteristic crack initiation sites by means of both experimental and numerical methods. Moreover, they investigated the influence of the contact COF and fastening forces on the initiation of cracks by means of the comparison of the different numerical results. Benhamena et al. [4] used 3-D FEA approach to analyses the effect of tightening torque on single bolted lap joint under fretting fatigue loading condition. In their work they also tried to monitor the contact status along with the potential location of fretting fatigue crack under different loading conditions. Chakherlou et al. [5] performed FE modelling of double shear lap joints subjected to cyclic load and compared with the experimental results under static loading condition in order to study the joints performance. In this paper fretting fatigue behaviour of SBLJ was monitored by developing a 3-D FE model, including location of initial crack, stress and slip distribution at contact interface between connected plates.

2 EXPERIMENTAL SET-UP

A SBLJ experimental specimen was configured by fastening two identical halves together through a single bolt, as schematically illustrated in Figure 1. Al 2024-T3 alloy panels of t= 4 mm thick were machined and cut to dimensions as described in the ASTM D5961/D5961M-01 standard, giving an overall length of 115 mm and a width of 40 mm, as shown in Figure 2. Circular fastener holes of 8.25 mm in diameter were drilled at the centre of the specimen width with a free edge distance of 15 mm. Socket head steel bolt (M8-8.8) was used to clamp the specimen halves and the tightening torque was applied with a calibrated torque

wrench. To avoid eccentricity in the applied load, which would lead to undesirable bending effects, end tabs of the same aluminium alloy 2024-T3 were bonded to each end of the test specimen as seen in Fig. 1.

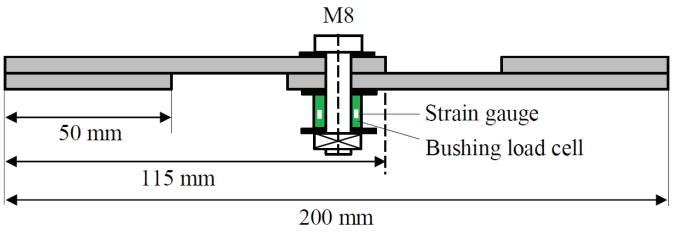

Fig. 1 Assembly view of the SBLJ specimen

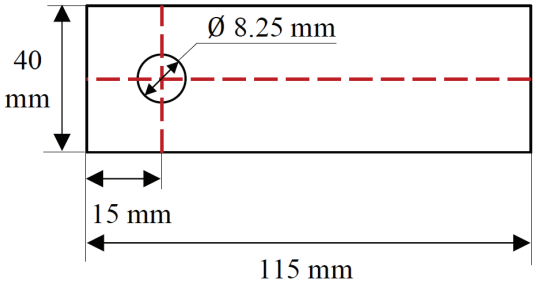

Fig. 2 Geometry of the SBLJ specimen

Specimens were prepared first by polishing lightly with sandpaper 800 grit followed by 1200 grit and finally cleaned with a pass by a cloth with acetone to remove all residual traces of debris remaining from this preparation process. Special care was taken for alignment of the specimens in the lower and upper grips as well as the relative alignment of the specimen halves to each other. For this purpose, a special fixture was used to assemble the SBLJ aiming to centring the bolt, load cell and plates to avoid having contact between inner side of the bolt hole and the bolt shank. The contact load was applied using a torque wrench after centring the Al plates, the load cell and the bolt using the special fixture.

Bolted joint specimens were tested with a servo hydraulic testing machine, according to the above-mentioned ASTM standard as depicted in Figure 3. In order to obtain experimentally the bolt clamping force in a bolted joint, there are different kinds of methods such as torque wrench method, angle control method and load cell strain gage method. In this research, the load cell and strain gage method was used, as it has better accuracy compared to other methods. The load cell comprised of a steel bush and two strain gauges positioned between the nut and the plate (see Fig. 1). This load cell was used to measure the compressive force due to the tightening torque. Two strain gauges were attached to the outer surface of the steel bush parallel to the bush axis as can be seen Fig. 3.

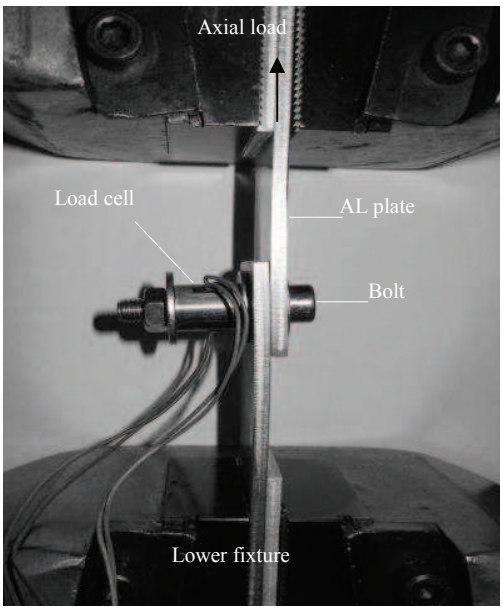

Fig. 3 SBLJ specimen mounted on universal servo-hydraulic fatigue machine

Figure 4 illustrates the variation of applied axial load versus displacement for SBLJ connection at F_{cl}= 14 kN clamping force. As shown in the figure, the elastic elongation of joint was used for validating FE model, which is elaborated later on. By increasing the axial load, the joint slips and eventually the bolt faces a shearing failure mode.

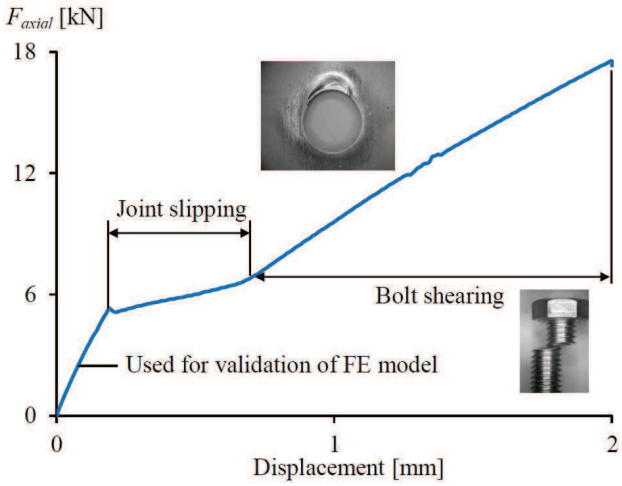

Fig. 4 Applied axial force versus displacement diagram for SBLJ

2.1 FE model

As mentioned earlier and shown above FE modelling approach is convenient methodology to investigate behaviour of fretting fatigue contact under different contact conditions. Therefore, using FE approach enhances the possibility to easily study more details compared to performed tests in a laboratory such as the distribution of slip at contact interface under different loading conditions. To this end, the preceding section focuses on characterizing fretting fatigue behaviour of SBLJ by means of 3-D FE modelling approach. In order to model SBLJ a few simplifications were made which may not cause any significant effect on the results. These simplifications can be listed as:

- A circular shape was used for the nut and bolt head. The socket shape of the bolt head was ignored.
- The washers were tied to the bolt head and nut because of having the same material elastic properties.
- Modelling of the bolt threads was ignored as there is no contact between threads and inner surface of hole.

A SBLJ model was generated using ABAQUS software. One half of experimental configuration needs to be model due to symmetry condition with respect to *x-y* plane in terms of both the geometry and loading. The model included two identical plates of Al 2024-T3, with a thickness of 4 mm and a 8.25 mm diameter hole as well as a M-8 steel bolt to clamp the plates. The dimensions of the modelled Al plates were the same as preformed SBLJ static test in Chapter 3. Isotropic material properties with elastic behaviour were defined to all components. Steel bolt, nut, load cell bush and washers with an elastic modulus of E= 210 GPa and a Poisson's ratio of ϑ = 0.33 and material properties with an elastic modulus of E= 72.4 GPa and a Poisson's ratio of ϑ = 0.33 was set for properties of the Al plates.

Figure 5 illustrates 3-D FE model of SBLJ along with the applied loading and boundary conditions, the same as static experimental set-up of SBLJ described in Chapter 3. The model consists of five different parts: two Al plates, three washers, bolt, nut and bushing load cell. Symmetric displacement boundary conditions were applied to the nodes on the symmetry planes. The loads were applied in two steps. Clamping contact load (F_{cl}) was applied in the first step to establish contact between contact pairs. In the second step axial stress was applied to the right side of Al plate. During the first step all three translational degrees of freedom (DOFs) at both left and right sides of the Al plates were restrained during applying clamping load. After applying clamping load the constraints at the right side of Al plate were removed and the axial load was applied instead as shown in Figure 5. 3-D structural 8-node linear brick, reduced integration, hourglass control (C3D8R) elements were used with the master-slave contact algorithm on the contact surface between Al plates interface, Al plates and the washers. The rest of contact pairs defined as a tie constant to reduce the computation time. As the vicinity of the bolt hole was the critical zone to be analyzed, density of the mesh was appropriately refined in this region as shown in Figure 5. The minimum mesh size at contact interface was 0.1 mm and increased gradually far from contact.

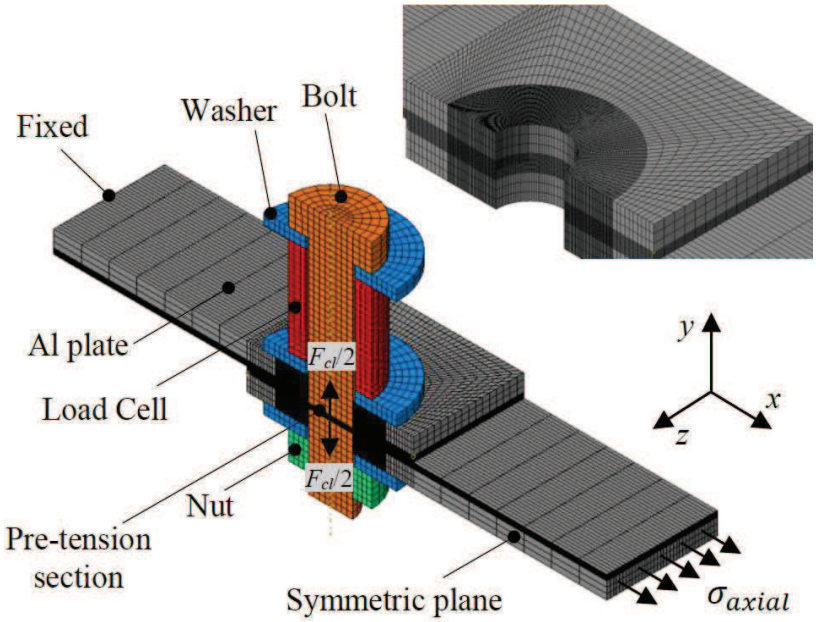

Fig. 5 FE model of SBLJ along with the applied loading and boundary conditions

A small sliding contact condition was used between the contact pair to transfer loads between the two bodies. The connecting contact surfaces were defined as a contact pair that enabled ABAQUS to determine if the contact pair was touching or separated. The contact region consisted of stick and slip regions under fretting fatigue loading condition. The stick region did not have a relative movement between contact surfaces. The slip region showed a small relative movement between contact surfaces on interface between two Al plates which is commonly observed in a fretting fatigue experiments. The penalty of friction was included in the contact pair to define the friction behaviour of the contact region as the Lagrange multiplier of friction did not converge in this particular SBLJ model. The coefficients of friction μ= 0.71 and μ= 0.2 were considered in this study for Al plates pairs and washer to Al plates, respectively.

In order to apply clamping load (F_{cl}) a pre-tension section in the bolt was defined as shown in Figure 5. When modelling the bolt with solid elements, the pre-tension section is defined as a surface in the bolt shank that effectively partitions the bolt into two regions. In continuum elements the pre-tension section is defined as a surface inside the fastener that “cuts” it into two parts. The pre-tension section can also be a group of surfaces for cases where a fastener is composed of several segments. Therefore, in the FE model the clamping load applied by applying a concentrated load, which is a self-equilibrating force carried across the pre-tension section in the bolt shank, to the pretension nodes.

3 FRETTING FATIGUE BEHAVIOUR OF SBLJ

Before investigation fretting fatigue behaviour of SBLJ it is essential to validate the FE model versus experimental results. Figure 6 illustrates the variation of axial load versus displacement for both FE model and static experimental test. Figures 7 (a) and (b) show the distribution of tangential and maximum principle stresses at contact interface between two Al plates. The high stress gradient is located at some distance from the hole near the contact edge (i.e. the side that the axial stress applied), which is also the potential location of initial crack in experimental results as reported in [9]. Figure 7 (c) indicates that the maximum frictional shear stress happens at almost the same distance as the maximum principle stress. Figure 7 (d) illustrates that the contact interface between two connected Al plates can be divided in three distinguished region namely, sticking, slipping and gapping.

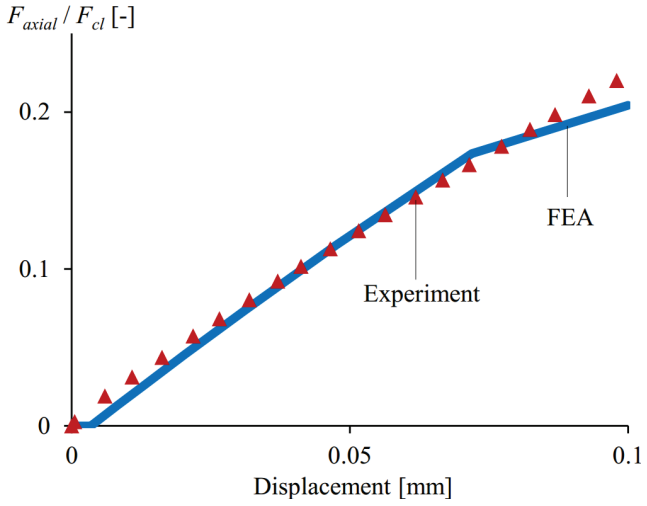

Fig. 6 Comparison between FE models and experimental results for F_{cl}= 14 kN

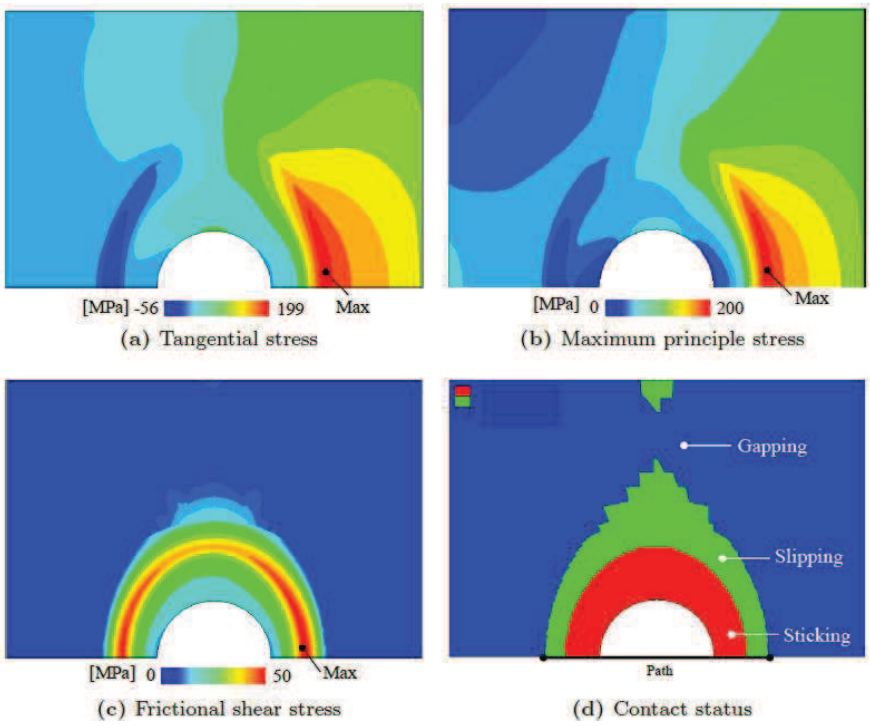

Fig. 7 Stress distribution at contact interface for SBLJ subjected to fretting fatigue loading condition at σ_{axial}= 20 MPa, F_{cl}= 14 kN and μ= 0.71

As investigated in author's' previous works the stress state is multiaxial for contact problems subjected to fretting fatigue loading condition. Therefore, by assuming that the damage causing stress is the equivalent multiaxial damage stress, the location of initial crack can be related to the location of maximum value of equivalent multiaxial damage stress (σ^*) at contact interface between two Al plates. More detailed information and validation of this criterion will be elaborated in [6-8].

Figures 8 (a) and (b) show the normalized equivalent multiaxial damage stress contour plot at contact interface between two Al plates and location of fretting fatigue crack initiation in SBLJ specimen for the same material taken from [9], respectively. As can be seen from Figures 8 (a), the maximum location of σ^* predicts the location of crack near the edge of contact, which is in good agreement with the experimental observation from literature [9]. Nonetheless, to find the exact location of initial crack the same loading and boundary conditions as the experimental test should be applied to the developed FE model for SBLJ.

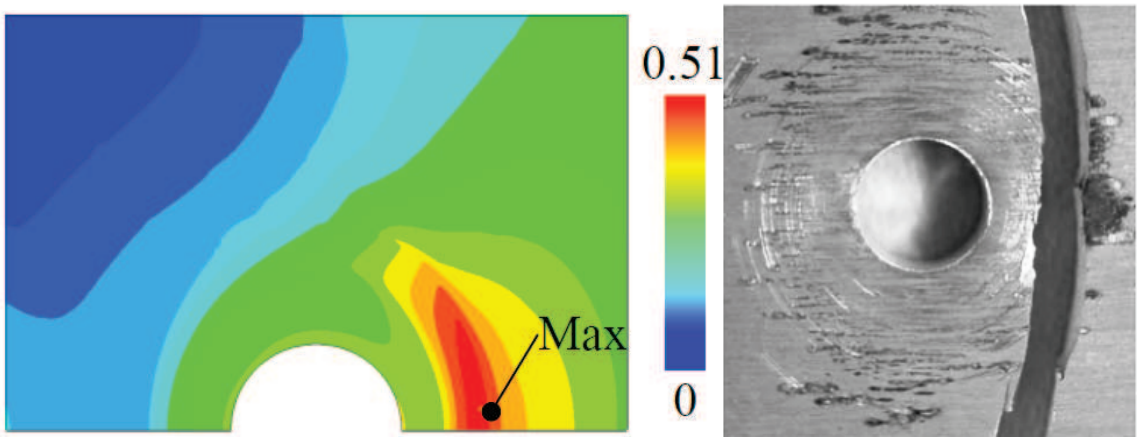

(a) σ^*/σ_{axial} (b)

Fig. 8 (a) Predicted location of initial crack in SBLJ connection subjected to fretting fatigue loading condition using FE approach at σ_{axial}= 20 MPa, F_{cl}= 14 kN and μ= 0.71, compared with the (b) experimental result

4 CONCLUSIONS

In this study, FE modelling approach was used to characterize fretting fatigue behaviour of SBLJ connection. It was found that FE modelling approach enhances the possibility to easily investigate more details compared to performed experimental tests in a laboratory and practical applications such as the distribution of relative slip amplitude, contact pressure or stresses at contact interfaces. It was shown that once the FE model is calibrated with help of experimental test or other calculation methods such as analytical one, it even offers the great capability of performing large parametric studies to check the influence of different parameters on behaviour of different structures subjected to fretting fatigue loading condition. To this end, using FE modelling approach the location of initial crack, stress and slip distribution at contact interface.

5 ACKNOWLEDGEMENTS

The authors wish to thank the Ghent University for the financial support received by the Special Funding, BOF (Bijzonder Onderzoeksfonds), in the framework of project (BOF 01N02410).

6 REFERENCES

[1] D. W. Heoppner, C. D. Elliot III, & M. W. Moesser, The role of fretting fatigue on aircraft rivet hole cracking, Technical report, DTIC Document, 1996.

[2] M. Szolwinski and T. Farris, Linking riveting process parameters to the fatigue performance of riveted aircraft structures, Journal of aircraft, 37(1), 130-137, 2000.

[3] R. Guo, R.C. Duan, G. Mesmacque, L. Zhang, A. Amrouche, Fretting fatigue behaviour of riveted al 6xxx components, Materials Science and Engineering: A, 483, 398-401, 2008.

[4] A. Benhamena, A. Talha, N. Benseddiq, A. Amrouche, G. Mesmacque and M Benguediab, Effect of clamping force on fretting fatigue behaviour of bolted assemblies: Case of couple steel aluminium. Materials Science and Engineering: A, 527(23), 6413-6421, 2010.

[5] T. Chakherlou and B. Abazadeh, Investigating clamping force variations in Al2024-T3 interference fitted bolted joints under static and cyclic loading, Materials & Design, 37,128-136, 2012.

[6] R. Hojjati-Talemi and M. A. Wahab, Fretting fatigue crack initiation lifetime predictor tool: Using damage mechanics approach, Tribology International 60(0), 176-186, 2013.

[7] R. Hojjati-Talemi and M. A. Wahab, Finite Element Analysis of Localized Plasticity in Al 2024-T3 Subjected to Fretting Fatigue, Tribology Transactions 55(6), 805-814, 2012.

[8] R. Hojjati-Talemi, M. A. Wahab, E. Giner, M. Sabsabi, Numerical estimation of fretting fatigue lifetime using damage and fracture mechanics, Tribology Letters, 52(1), 11-25, 2013.

[9] S. Wagle and H. Kato, Ultrasonic detection of fretting fatigue damage at bolt joints of aluminium alloy plates, International Journal of Fatigue, 31(8),1378-1385, 2009.